*Structural Engineering and Mechanics, Vol. 17, No. 6 (2004) 863-878* 863
DOI: http://dx.doi.org/10.12989/sem.2004.17.6.863

# Bond strength modeling for corroded reinforcement in reinforced concrete

Xiaohui Wang† and Xila Liu‡

*A0110021#, Department of Civil Engineering, Shanghai Jiaotong University, Minhang, Shanghai, 200240, P.R. China*

*(Received October 23, 2002, Accepted December 10, 2003)*

**Abstract.** Steel corrosion in reinforced concrete structures leads to concrete cover cracking, reduction of bond strength, and reduction of steel cross section. Among theses consequences mentioned, reduction of bond strength between reinforcement and concrete is of great importance to study the behaviour of RC members with corroded reinforcement. In this paper, firstly, an analytical model based on smeared cracking and average stress-strain relationship of concrete in tension is proposed to evaluate the maximum bursting pressure development in the cover concrete for noncorroded bar. Secondly, the internal pressure caused by the expansion of the corrosion products is evaluated by treating the cracked concrete as an orthotropic material. Finally, bond strength for corroded reinforcing bar is calculated and compared with test results.

**Key words:** corrosion; bond strength; smeared cracking; corrosion pressure.

## 1. Introduction

Reinforcement corrosion is one of the major causes of reinforced concrete structure deterioration. Corrosion may affect: (a) The steel, due to the reduction of both the steel cross section and the mechanical properties (Almusallam 2001); (b) The concrete, due to the expansion of corrosion products, cracking, splitting and even delaminating (Andrade *et al.* 1993, Molina *et al.* 1993); (c) The bond strength between steel and concrete, due to the accumulation of corrosion products around the steel, deteriorating or lost. Among the consequences mentioned above, many research works (Al-Sulaimani *et al*. 1990, Cabrera and Ghoddoussi 1992, Stanish *et al.* 1999, Amleh and Mirza 1999, Mangat and Elgarf 1999, Auyeung *et al.* 2000, Zhao and Jin 2002) focused on bond behavior of corroded reinforcement. However, these works are experimental. The empirical formulae that describe what influence corrosion has on the bond strength are based on the corresponding test results.

Recently, general models for the prediction of bond strength for corroded bars have been proposed by Lundgren (2002) and Coronelli (2002), respectively. Lundgren (2002) assumes corrosion products as a corrosion layer. Bond model is combined with the modeling of the corrosion layer, and a three-dimensional finite element program DIANA is used. Coronelli (2002) proposes a model

† Ph.D. Student
‡ Professor

to predict both the pressure around a corroded bar and the bond strength at the onset of pullout in an anchorage. Before corrosion cracking of the cover concrete, the maximum pressure at bond failure is taken as the maximum bursting capacity for noncorroded bars, where the maximum bursting capacity is evaluated with the limit analysis method proposed by Tepfers (1979) for noncorroded bars; the pressure exerted by the expansion of corrosion products is evaluated by modeling the concrete cover as a beam, which has a cross section defined by the cover in the two orthogonal directions and rests on evenly spaced supports that represent the confinement exerted by the surrounding concrete. However, softening behaviour of concrete is not considered in the limit analysis method suggested by Tepfers (1979), whereas concrete cover can still maintain some residual strength after its tensile capacity is exceeded; meanwhile, the residual confinement pressure is evaluated from the tests by Baldwin and Clark (Coronelli 2002) after the splitting strength of concrete cover is exhausted by the expansion of the corrosion products.

In the present paper, firstly, an analytical model is proposed to evaluate the maximum pressure development in the confined concrete before corrosion cracking of the concrete cover. Smeared cracks are assumed to form in the radial direction as hoop stresses exceed the tensile capacity of concrete; therefore, the average hoop tensile strain integrated over the perimeter represents the sum of the true, discrete crack openings. Constant radial displacement is assumed in partly cracked concrete. After corrosion cracking, the residual confinement pressure is calculated in association with different corrosion levels. Secondly, corrosion pressure is evaluated by treating the cracked concrete as an orthotropic material before and after corrosion cracking. Smeared cracks are assumed and the average stress-strain relationships of cracked concrete in two principal directions are used. Finally, a modified model proposed by Coronelli (2002) for splitting bond failure is used to evaluate bond strength for corroded bars.

## 2. Bar-concrete pressure $p(x)$ for corroded bars

Before corrosion cracking of the cover concrete, the maximum pressure $p(x)$ for corroded bars can reach the maximum bursting capacity for noncorroded bars (Coronelli 2002); after corrosion cracking, the residual confinement pressure is evaluated in association with different corrosion levels. Therefore, the maximum bar-concrete pressure for noncorroded bars is evaluated firstly, then the bar-concrete pressure for corroded bars after corrosion cracking is calculated.

### *2.1 Bar-concrete pressure for noncorroded bars*

The bond between steel and concrete consists of three mechanisms: adhesion, friction and mechanical interlock. When a ribbed bar is pulled out of the concrete, its bond strength mainly originates from mechanical interaction between the steel ribs and the surrounding concrete. A splitting crack occurs if the tensile strength of concrete is reached. Tepfers (1979) treated this problem as a thick-walled cylinder subjected to internal radial pressure. Later several research works (Reinhardt and Van der Veen 1992, Olofsson *et al.* 1995, Noghabai 1996, Gambarova *et al.* 1994, Gambarova and Rosati 1997, Nielsen and Bicanic 2002) have been carried out on the basis of the idea of Tepfers (1979). In order to consider the softening behaviour of concrete, the thick-walled cylinder is divided into two rings: an uncracked outer ring and a partly cracked inner ring. Different concrete tensile softening models have been used in the cracked inner ring: a power-law model

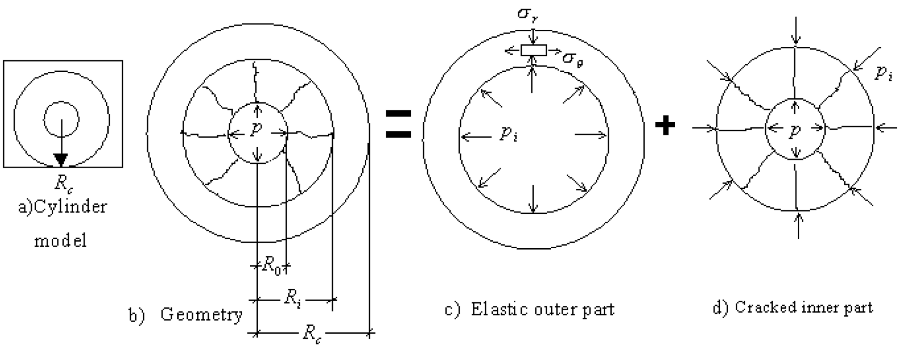


Fig. 1 Concrete cylinder with partly cracked inner part

(Reinhardt and Van der Veen 1992), a linear softening curve (Olofsson *et al.* 1995, Noghabai 1996), and an elasto-cohesive model (Gambarova *et al.* 1994, Gambarova and Rosati 1997). However, theses models have a common characteristic: they are related to the number of assumed radial cracks. Therefore, the results of the problem are associated with the number of assumed radial cracks. But it is different to determine the number of radial cracks in real concrete structures because there are thousands of microcracks and cracks in cracked concrete.

In the present paper, the methodology proposed by Tepfers (1979) is also used; the problem of determining the internal radial pressure $p$ is divided into two parts, see Fig. 1, wherein the reinforcing bar of initial radius $R_0$ is embedded in concrete with outer radius $R_c$, the concrete cover dimension measured from the center of the bar to the nearest surface of concrete. $R_i$ defines the crack front, where the hoop stresses equal to the tensile strength of concrete $f_{ct}$.

Simple equilibrium conditions written along any radially cracked section give the following equation, by introducing the softening behaviour of concrete:

$$p \cdot R_0 = p_i \cdot R_i + \int_{R_0}^{R_i} \sigma_\theta dr \tag{1}$$

where the hoop stress $\sigma_\theta$ is assumed to vary only in the radial direction.

The pressure $p_i$ can be obtained from the solution $\sigma_\theta|_{r = R_i} = f_{ct}$ of the elastic out part, see Fig. 1(c):

$$p_i = f_{ct} \cdot \frac{R_c^2 - R_i^2}{R_c^2 + R_i^2} \tag{2}$$

To obtain $\sigma_\theta$ in the cracked part, see Fig. 1(d), the displacement and stresses are considered in this cracked part. Smeared cracking is assumed to form in the radial direction as hoop stresses exceed the tensile capacity of concrete; therefore, the formulation is written in terms of average stresses and strains; and the average hoop tensile strain $\varepsilon_\theta$, integrated over the perimeter, represents the sum of the true, discrete crack openings (Pantazopoulou and Papoulia 2001). As a result, the total tangential elongation $\delta_t$ at a radial distance $r$ from the center of thick-walled cylinder, which is expressed as the sum of $n_c$ crack widths plus the linear-elastic extension of the concrete between the cracks (Reinhardt and Van der Veen 1992, Olofsson *et al.* 1995, Noghabai 1996, Gambarova *et al.* 1994, Gambarova and Rosati 1997, Nielsen and Bicanic 2002), where $n_c$ is the assumed number of radial cracks, can be expressed as following:

$$\delta_t = 2\pi \cdot r \cdot \varepsilon_\theta \tag{3}$$

At a radial distance $R_i$, the tensile strength of concrete $f_{ct}$ is reached and no cracks exist. Then, the total tangential elongation $\delta_t$ is

$$\delta_t = 2\pi R_i \varepsilon_\theta \approx 2\pi R_i \frac{f_{ct}}{E_0} = 2\pi R_i \varepsilon_{ct} \tag{4}$$

where the Poisson's effect is neglected; and $E_0$ is the initial elastic modulus of concrete; $\varepsilon_{ct}$ is the tensile strain capacity of concrete, $\varepsilon_{ct} = f_{ct}/E_0$.

The associated radial displacement $u_r = R_i \cdot \varepsilon_{ct}$ is assumed to be constant (Reinhardt and Van der Veen 1992, Olofsson *et al.* 1995, Noghabai 1996, Gambarova *et al.* 1994, Gambarova and Rosati 1997). Considering the compatibility between the cracked and uncracked parts, the following equation can be obtained:

$$\delta_t = 2\pi r \varepsilon_\theta = 2\pi R_i \varepsilon_{ct} \tag{5}$$

Thus, the average hoop strain $\varepsilon_\theta$ at a radial distance $r$ is given by

$$\varepsilon_\theta = \frac{R_i}{r} \cdot \varepsilon_{ct} \tag{6}$$

In Eq. (6) $\varepsilon_\theta$ is related to the constitutive relation of concrete in tension. The following average stress-strain relationship of concrete in tension (Fig. 3) is used (Hsu 1996), see Fig. 2.

$$\sigma_\theta = E_0 \cdot \varepsilon_\theta \qquad \varepsilon_\theta \le \varepsilon_{ct} \tag{7a}$$

$$\varepsilon_\theta = f_{ct} \cdot \left(\frac{\varepsilon_{ct}}{\varepsilon_\theta}\right)^{0.4} \qquad \varepsilon_\theta > \varepsilon_{ct} \tag{7b}$$

where $E_0$ is taken as $3875\sqrt{f_c'}$ ($f_c'$ and $\sqrt{f_c'}$ are in Mpa); $f_{ct}$ is taken as $0.33\sqrt{f_c'}$ ($f_c'$ and $\sqrt{f_c'}$ are in Mpa); $f_c'$ is the compressive strength of concrete.

According to Eq. (6), it is evident that $\varepsilon_\theta > \varepsilon_{ct}$. Substituting Eq. (6) into Eq. (7b), then $\sigma_\theta$ in the cracked part is given by

$$\varepsilon_\theta = f_{ct} \cdot \varepsilon_{ct}^{0.4} \cdot \left(\frac{r}{R_i \varepsilon_{ct}}\right)^{0.4} = f_{ct} \cdot R_i^{-0.4} \cdot r^{0.4} \tag{8}$$

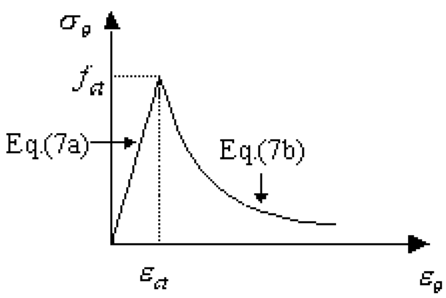


Fig. 2 Average stress-strain curve of cracked concrete (Hsu 1996)

Substituting Eq. (2) and Eq. (8) into Eq. (1), it simplifies to

$$p \cdot R_0 = R_i \cdot f_{ct} \cdot \frac{R_c^2 - R_i^2}{R_c^2 + R_i^2} + f_{ct} \cdot R_i^{-0.4} \cdot \frac{R_i^{1.4} - R_0^{1.4}}{1.4} \tag{9}$$

Differentiation of Eq. (9) with respect to $R_i$ gives

$$\frac{d\left(\frac{p \cdot R_0}{f_{ct}}\right)}{dR_i} = \frac{R_c^4 - R_i^4 - 4R_i^2 \cdot R_c^2}{(R_c^2 + R_i^2)^2} + \frac{1 + 0.4 \cdot R_0^{1.4} \cdot R_i^{-1.4}}{1.4} \tag{10}$$

Eq. (10) is put to zero, and solved numerically for $R_i$. Taking the corresponding $R_i$ into Eq. (9), the maximum bar-concrete pressure $p_{\max}$ for noncorroded reinforcement can be obtained.

### 2.2 Bar-concrete pressure for corroded bars after corrosion cracking

When the concrete cover is cracked, the stirrups and the concrete remaining around the bar still develop some residual confining action (Giuriani *et al.* 1991, Coronelli 2002). Hence, a residual confinement pressure $p_{res}$ is still present. In the case where no stirrups are provided, the confinement pressure can be calculated by summing the contribution of the residual tensile strength of cracked concrete (Giuriani *et al.* 1991).

To determine the residual confinement pressure $p_{res}$, the method used in section 2.1 is still adopted. Now, the equilibrium equation similar to Eq. (1) is given by

$$p_{res} \cdot R_0 = \int_{R_0}^{R_c} \sigma_\theta dr \tag{11}$$

Smeared cracking is also assumed and Poisson's effect is neglected. At the edge of the cracked concrete ring, $r = R_c$, the hoop strain is assumed to be $\varepsilon_x$, and the associated radial displacement $u_r = R_c \cdot \varepsilon_x$ is assumed to be constant. Thus, the average hoop strain at a distance $r$ is given by

$$\varepsilon_\theta = \frac{R_c}{r} \cdot \varepsilon_x \tag{12}$$

Using the average stress-strain relationship of concrete in tension, $\sigma_\theta$ in Eq. (11) is given by

$$\sigma_\theta = f_{ct} \cdot \varepsilon_{ct}^{0.4} \cdot \left(\frac{r}{R_c \cdot \varepsilon_x}\right)^{0.4} \tag{13}$$

Substituting Eq. (13) into Eq. (11), it simplifies to

$$p_{res} \cdot R_0 = f_{ct} \cdot \varepsilon_{ct}^{0.4} \cdot R_c^{-0.4} \cdot \varepsilon_x^{-0.4} \cdot \frac{R_c^{1.4} - R_0^{1.4}}{1.4} \tag{14}$$

When the hoop strain $\varepsilon_x$ at $r = R_c$ is given, the corresponding residual confinement pressure $p_{res}$ can be obtained from Eq. (14). In this paper, this hoop strain $\varepsilon_x$ is related to the corrosion level. This problem is solved in the following.

## 3. Corrosion pressure $p_{cor}(x)$ for corroded bars

### 3.1 Corrosion pressure for corroded bars before corrosion cracking

#### 3.1.1 Definition of the mechanical problem

The method used in this part is similar to that used in section 2. In this approach, the evolution of internal pressure is an output of the solution rather than the controlling parameter. The controlling variable is a prescribed radial displacement $u_r|_{r=R_0}$ at the inner boundary of the concrete cover layer. This prescribed radial displacement is related to the volumetric expansion of the rusting reinforcement (Pantazopoulou and Papoulia 2001). The problem is modeled with reference to Fig. 3, wherein $R_0$ is the initial radius of reinforcing bar; $R_s$ is the reduced radius of reinforcing bar; $R_c$ is the outer radius of concrete cover measured from the center of the bar to the nearest surface of concrete; $R_r$ defines the rust front; $R_i$ defines the crack front. The prescribed radial displacement $u_r|_{r=R_0}$ is given by $u_r|_{r=R_0} = R_r - R_0$.

Assuming uniform corrosion on the bar surface, the attack penetration depth or radius loss of the bar is defined as $x$. Then the reduced radius of bar $R_s$ is given by $R_s = R_0 - x$. The corresponding volume of the steel consumed per unit length of the bar is given by $\Delta V_s = \pi R_0^2 - \pi R_s^2 = 2\pi R_0 x - \pi x^2$. And the corresponding volume of accumulated rust products on the bar perimeter $\Delta V_r$ is $\Delta V_r = n\Delta V_s$, where $n$ is the ratio between the volume of rust products and virgin steel, the value of $n$ is taken as 1.7~6.15 according to different corrosion products (Lundgren 2002).

Considering a part of the corrosion products flows away from the bar surface through the cracks and pores of concrete toward the free surface, the volume of accumulated rust products is $\Delta V_r = n\Delta V_s = \pi t_r(2R_s + t_r) + \pi \cdot u_r|_{r=R_0} \cdot (R_i - R_r)$ (Pantazopoulou and Papoulia 2001), from which, with $u_r|_{r=R_0} = R_r - R_0$ and $R_r = R_s + t_r$, where $t_r$ is the thickness of rust layer, it follows that

$$t_r = \frac{n(2R_0x - x^2) + x \cdot (R_i - R_0 + x)}{R_i + R_0} \tag{15}$$

Then the prescribed radial displacement $u_r|_{r=R_0}$ is given by

$$u_r|_{r=R_0} = R_r - R_0 = t_r - x = \frac{(n-1) \cdot (2R_0x - x^2)}{R_i + R_0} \tag{16}$$

When the prescribed radial displacement $u_r|_{r=R_0}$ is given, attention is paid to the solution of the problem in Fig. 3. The problem is divided into two parts: elastic outer and cracked inner part, see

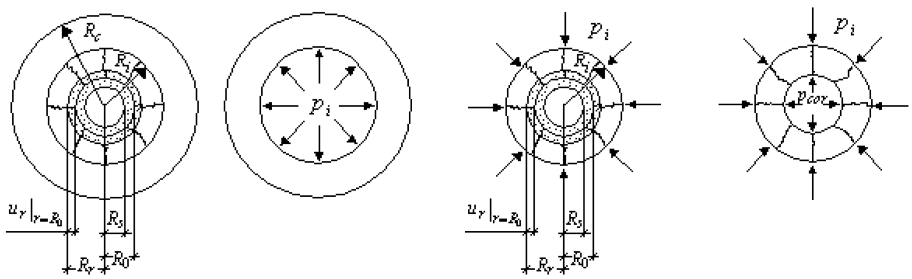


Fig. 3 Concrete cylinder with the prescribed radial displacement $u_r|_{r=R_0}$

Fig. 3(b) and 3(c). In the elastic outer part, there is sound concrete, whereas sound concrete is treated as an isotropic material. Therefore, the internal pressure $p_i$ is also given by Eq. (2). For the cracked inner part, firstly, smeared cracking is assumed; as a result, the formulation is written in terms of average stresses and strains. Secondly, the cracked concrete is treated as an anisotropic elastic material. The governing equation of the problem is written as a differential equation for the radial displacement $u_r$ (Pantazopoulou and Papoulia 2001)

$$\frac{d^2u_r}{dr^2} + \frac{1}{r} \cdot \frac{du_r}{dr} - \frac{u_r}{r^2} \cdot \frac{E_\theta}{E_r} = 0 \tag{17}$$

where $E_r$, $E_\theta$ are the secant stiffnesses of the cracked concrete in the radial and hoop directions. The corresponding radial, hoop strains and stresses are given by

$$\varepsilon_r = \frac{du_r}{dr}, \qquad \varepsilon_\theta = \frac{u_r}{r} \tag{18a,b}$$

$$\sigma_r = \frac{1}{1 - \nu_{r\theta}\nu_{\theta r}}(E_r\varepsilon_r + \nu_{r\theta}E_\theta\varepsilon_\theta), \quad \sigma_\theta = \frac{1}{1 - \nu_{r\theta}\nu_{\theta r}}(E_\theta\varepsilon_\theta + \nu_{\theta r}E_r\varepsilon_r) \tag{19a,b}$$

where the Poisson's ratios $\nu_{r\theta}$ and $\nu_{\theta r}$ are related by virtue of the requirements of anisotropic elasticity as $\nu_{\theta r}E_r = \nu_{r\theta}E_\theta$ (Pantazopoulou and Papoulia 2001). As the secant slope of the stress-strain relationships of cracked concrete in principal directions defines stiffnesses, the constitutive laws of concrete must be known.

### 3.1.2 Modeling of material behaviour

Hoop and radial directions are principal directions because of the assumed axisymmetry of the problem. The hoop stresses $\sigma_\theta$ typically are tensile, whereas the radial stresses $\sigma_r$ are compressive. Smeared cracks are assumed to form in the radial direction as hoop stresses exceed the tensile capacity of concrete $f_{ct}$.

The following stress-strain relationships of cracked concrete are used (Pantazopoulou and Papoulia 2001, Hsu 1996), see Fig. 4:

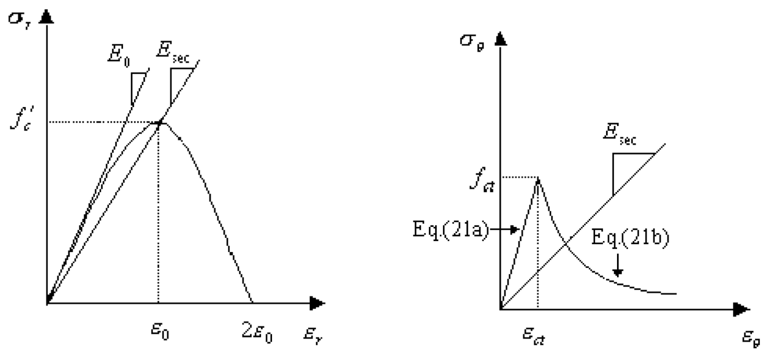


Fig. 4 Stress-strain relationships of cracked concrete in principal directions. a) Principal compression (Pantazopoulou and Papoulia 2001); b) Principal tension (Hsu 1996)

concrete in compression (Pantazopoulou and Papoulia 2001, Fig. 4a)

$$\sigma_r = f_c'\left[2\cdot\frac{\varepsilon_r}{\varepsilon_0}-\left(\frac{\varepsilon_r}{\varepsilon_0}\right)^2\right] \tag{20}$$

concrete in tension (Hsu 1996, Fig. 4b)

$$\sigma_\theta = E_0\cdot\varepsilon_\theta \qquad \varepsilon_\theta\le\varepsilon_{ct} \tag{21a}$$

$$\sigma_\theta = f_{ct}\cdot\left(\frac{\varepsilon_{ct}}{\varepsilon_\theta}\right)^{0.4} \qquad \varepsilon_\theta>\varepsilon_{ct} \tag{21b}$$

where $f_c'$ is the uniaxial compressive strength of concrete and $\varepsilon_0$ is the corresponding axial compressive strain, $\varepsilon_0 = 2f_c'/E_0$; $E_0$ and $\varepsilon_{ct}$ are the same values as in Fig. 2.

#### 3.1.3 Solution of the problem

In order to obtain the unknown corrosion pressure $p_{cor}$, the crack front $R_i$ in Fig. 3 and the radial displacement $u_r(r)$ in Eq. (17), a finite-difference scheme is established with the radial direction discretized into $N+1$ equidistant nodes (i.e., $N$ intervals with length $h = (R_i-R_0)/N$). The first node, $i=0$, is located at $r=R_0$, and the last node, $i=N$, is located at $r=R_i$. The corresponding boundary conditions are

$$u_r\big|_{r=R_0} = R_r-R_0, \qquad \sigma_\theta\big|_{r=R_i} = f_{ct} \tag{22a,b}$$

Using a central-difference scheme to express the derivatives at the point $r=r_i$ in discrete form (Pantazopoulou and Papoulia 2001)

$$\frac{du_r}{dr} = \frac{u_{r,i+1}-u_{r,i-1}}{2h}, \qquad \frac{d^2u_r}{dr^2} = \frac{u_{r,i+1}-2u_{r,i}+u_{r,i-1}}{h^2} \tag{23a,b}$$

and for $i = 0, 1, 2, \ldots, N$. Eq. (17) is written in terms of nodal displacements

$$-u_{r,i-1}\left(\frac{1}{h^2}-\frac{1}{2r_ih}\right)+u_{r,i}\left(\frac{2}{h^2}+\frac{1}{r_i^2}\cdot\frac{E_{\theta,i}}{E_{r,i}}\right)-u_{r,i+1}\left(\frac{1}{h^2}+\frac{1}{2r_ih}\right) = 0 \tag{24}$$

Setting $u_{r,0} = u_r\big|_{r=R_0} = R_r-R_0$, Eq. (24) for $i=1$ becomes

$$u_{r,1}\left(\frac{2}{h^2}+\frac{1}{r_1^2}\cdot\frac{E_{\theta,1}}{E_{r,1}}\right)-u_{r,2}\left(\frac{1}{h^2}+\frac{1}{2r_1h}\right) = (R_r-R_0)\left(\frac{1}{h^2}-\frac{1}{2r_1h}\right) \tag{25}$$

where $u_r\big|_{r=R_0} = R_r-R_0$ is given by Eq. (16).

The discretized form of Eq. (22b) is

$$\frac{u_{r,N+1}-u_{r,N-1}}{2h}\cdot\nu_{r\theta,N}E_{\theta,N}+E_{\theta,N}\frac{u_{r,N}}{r_N} = f_{ct}\left(1-\frac{\nu_{r\theta,N}^2E_{\theta,N}}{E_{r,N}}\right) \tag{26a}$$

then

$$u_{r,N+1} = u_{r,N-1} + \frac{2hf_{ct}}{\nu_{r\theta,N}E_{\theta,N}}\left(1 - \frac{\nu_{r\theta,N}^2 E_{\theta,N}}{E_{r,N}}\right) - \frac{2hu_{r,N}}{\nu_{r\theta,N}r_N} \tag{26b}$$

Substituting Eq. (26b) into Eq. (24) for $i = N$ (i.e., $r_N = R_i$), it simplifies to

$$-\frac{2}{h^2}u_{r,N-1} + u_{r,N}\left[\frac{2}{h^2} + \frac{1}{r_N^2}\frac{E_{\theta,N}}{E_{r,N}} + \left(\frac{1}{h^2} + \frac{1}{2r_N h}\right)\cdot\frac{2h}{\nu_{r\theta,N}r_N}\right] - a_N = 0 \tag{27}$$

where $a_N = \left(\frac{1}{h^2} + \frac{1}{2r_N h}\right)\cdot\frac{2hf_{ct}}{\nu_{r\theta,N}E_{\theta,N}}\cdot\left(1 - \frac{\nu_{r\theta,N}^2 E_{\theta,N}}{E_{r,N}}\right)$.

Eq. (24), Eq. (25) and Eq. (27) can be written as an $N \times N$ tridiagonal system of equations $[K][u_r] = [B]$ with $[K]$, $[u_r]$ and $[B]$ shown in Appendix.

The pressure exerted by the corroding bar on the surrounding concrete cover is obtained by calculating the radial stress at $r = R_0$ (Fig. 3c)

$$p_{cor} = \sigma_r\big|_{r=R_0} = \frac{1}{\nu_{r\theta,0}\nu_{\theta r,0}}\left(E_{r,0}\cdot\frac{u_{r,1} - u_{r,-1}}{2h} + \nu_{r\theta,0}E_{\theta,0}\frac{u_{r,0}}{R_0}\right) \tag{28}$$

where the displacement $u_{r,-1}$ is obtained from Eq. (24) for $i = 0$ (i.e., at $r = R_0$)

$$u_{r,-1} = \left(\frac{1}{h^2} - \frac{1}{2R_0 h}\right)^{-1}\cdot\left[u_{r,0}\left(\frac{2}{h^2} + \frac{1}{R_0^2}\frac{E_{\theta,0}}{E_{r,0}}\right) - u_{r,1}\left(\frac{1}{h^2} + \frac{1}{2R_0 h}\right)\right] \tag{29}$$

Eq. (24), Eq. (25) and Eq. (27) must be combined with Eq. (30), which is the equilibrium condition written along any radially cracked section of the cracked inner part, see Fig. 3(d), to solve unknown variables for different attack penetration depth $x$.

$$-p_{cor}\cdot R_0 = p_i\cdot R_i + h\cdot\sum_{i=0}^{N}\sigma_{\theta,i} \tag{30}$$

where the sign "–" is used to consider that the corrosion pressure $p_{cor}$ or the radial stress $\sigma_r\big|_{r=R_0}$ calculated from Eq. (28) is compressive.

### 3.2 Corrosion pressure for corroded bars after corrosion cracking

When $R_i = R_c$, the concrete cover is fully cracked. The corresponding attack penetration depth $x$ is defined as $x_{cr}$. From this stage onward, the whole concrete cover is treated as an anisotropic elastic material. The governing equation of the problem, the corresponding radial, hoop strains and stresses and the stress-strain relationships of cracked concrete are the same as these in section 3.1. Now, the whole clear cover is discretized into $N + 1$ equidistant nodes (i.e., $N$ intervals with length $h = (R_c - R_0)/N$). The first node, $i = 0$, is located at $r = R_0$, and the last node, $i = N$, is located at $r = R_c$. The corresponding boundary conditions are

$$u_r\big|_{r = R_0} = R_r - R_0, \qquad \sigma_r\big|_{r = R_c} = 0 \tag{31a,b}$$

Substituting the discretized form of Eq. (31b) into Eq. (24) for $i = N$ (i.e., $r_N = R_c$, it simplifies to (Pantazopoulou and Papoulia 2001)

$$-\frac{2}{h^2}u_{r,N-1} + u_{r,N}\left[\frac{2}{h^2} + \frac{1}{r_N^2}\frac{E_{\theta,N}}{E_{r,N}} + \nu_{r\theta,N}\frac{E_{\theta,N}}{E_{r,N}}\cdot\frac{2h}{r_N}\cdot\left(\frac{1}{h^2} + \frac{1}{2r_Nh}\right)\right] = 0 \tag{32}$$

For a given $x$ ($x > x_{cr}$), the unknown radial displacements are obtained by solution of a combination of equations Eq. (24), Eq. (25) and Eq. (32), and the corresponding corrosion pressure $p_{cor}$ is given by the following equation

$$-p_{cor}\cdot R_0 = h\cdot\sum_{i=0}^{N}\sigma_{\theta,i} \tag{33}$$

where $h = (R_c - R_0)/N$.

The corresponding hoop strain $\varepsilon_x$ at $r = R_c$ is given by

$$\varepsilon_x = \frac{u_{r,N}}{R_c} \tag{34}$$

Taking Eq. (34) into Eq. (14), the residual confinement pressure $p_{res}$ at a given attack penetration depth $x(x > x_{cr})$ can be obtained.

## 4. Bond strength for corroded reinforcement

The following model, originally proposed by Cairns and Abdullah (1996) and modified by Coronelli (2002) to consider corroded bars, is used to calculate bond strength for corroded reinforcement for splitting bond failure

$$\tau_{bu}(x) = k(x)p(x) + \tau_b^0(x) + \mu(x)p_{cor}(x) \tag{35}$$

where $p(x)$: maximum confinement pressure for corroded bars at bond failure

when $x \le x_{cr}$ $p(x) = p_{\max}$ where $p_{\max}$ is calculated by Eq. (9) and Eq. (10);

when $x > x_{cr}$ $p(x) = p_{res}$ where $p_{res}$ is calculated by Eq. (14).

$p_{cor}(x)$: corrosion pressure, obtained from section 3 for different values of $x$;

$k(x)$: coefficient, given by Cairns and Abdullah (1996) as following

$$k(x) = k_r\cdot A_r\cdot tg(\delta + \phi)/(I\cdot\pi\cdot d\cdot s_r) \tag{36}$$

for an annular rib, $k_r = 1$, $I = dh_r$, $A_r = \pi dh_r$ $\quad k(x) = tg(\delta + \phi)/(d\cdot s_r)$ (36a)

for crescent-shaped ribs, given by Coronelli (2002) as

$$k(x) = 0.8k_r\cdot tg(\delta + \phi)/\pi \tag{36b}$$

$\tau_b^o(x)$: non-splitting components of bond strength (Cairns and Abdullah 1996)

$$\tau_b^o(x) = k_r A_r f_{coh} \cdot [ctg\delta + tg(\delta + \phi)]/(\pi \cdot d \cdot s_r) \tag{37}$$

$\mu(x)$: friction coefficient, given by Coronelli (2002) as

$$\mu(x) = tg\phi = 0.37 - 0.26(x - x_{cr}) \tag{38}$$

$f_{coh} = f_{coh}(x)$: adhesion strength, given by Coronelli (2002) as

$$f_{coh}(x) = 3.41 - 21.21(x - x_{cr}) \tag{39}$$

$A_r = A_r(x)$: rib area in the plane at right angles to bar axis

for an annular rib, $$A_r(x) = \pi \cdot d \cdot (h_r - x) \tag{40a}$$

for crescent-shaped ribs, $$A_r(x) = 0.5\pi \cdot [d(h_{rave} - x) - (h_{rave} - x)^2]/\sin\beta \tag{40b}$$

$d$: diameter of reinforcing bar;
$s_r$: longitudinal spacing of transverse ribs. For crescent-shaped ribs, the value of $s_r$ is suggested to take as $d/tg\beta$;
$k_r$: number of transverse ribs at section, $k_r = 2$ for crescent-shaped ribs;
$\beta$: inclination of rib to bar axis, suggested value (Plizzari *et al.* 1998) is $\beta = 57^o \sim 60^o$;
$h_r$: height of transverse rib, for an annular rib, $h_r$ is a constant;
$h_{rave}$: average rib height for crescent-shaped ribs, suggested value (Plizzari *et al.* 1998) is $h_{rave} = (1/19 - 1/21) \cdot d$;
$\delta$: inclination of bearing face of rib to bar axis, suggested value (Cairns and Abdullah 1996) is $\delta = 35^o \sim 45^o$;
$\phi = \phi(x)$: friction angle between reinforcing bar and concrete.

## 5. Numerical results of the models

### 5.1 Comparison with Tepfers' classic solutions

The maximum bursting capacity $p_{\max}$ for noncorroded bars is evaluated by Tepfers (1979) in three stages: a linear-elastic stage (lower bound); a plastic stage (upper bound); and an intermediate partly cracked elastic stage. In Fig. 5, the relative maximum pressure $p_{\max}/f_{ct}$ is depicted as a function of the relative cover thickness $c/d$, where $c$ is the clear concrete cover. The solution of Eq. (9) and Eq. (10) for noncorroded bar is compared with Tepfers' solutions. It is seen from Fig. 5 that the proposed model falls in between the partly cracked elastic stage and the plastic stage as pointed out by Tepfers.

### 5.2 Comparison with test results of Mangat and Elgarf (1999)

An experiment taken from the literature is used (Mangat and Elgarf 1999). Reinforced concrete beams of 910 mm length, and rectangular cross-section 150 mm deep and 100 mm wide were used.

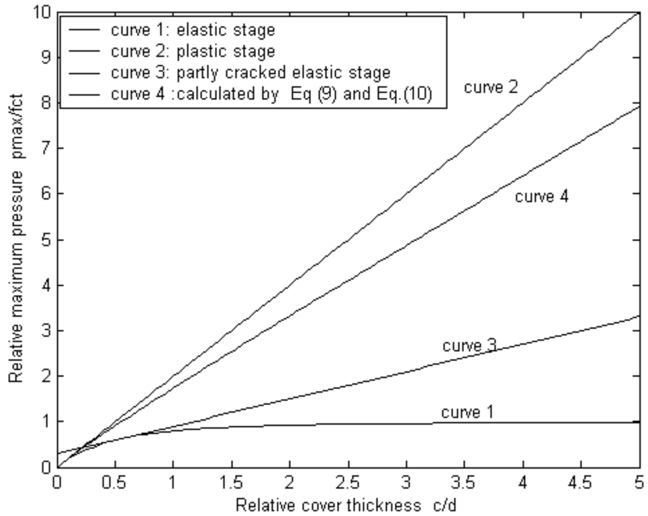


Fig. 5 The relative maximum $p_{max}/f_{ct}$ as a function of the relative cover thickness *c/d*

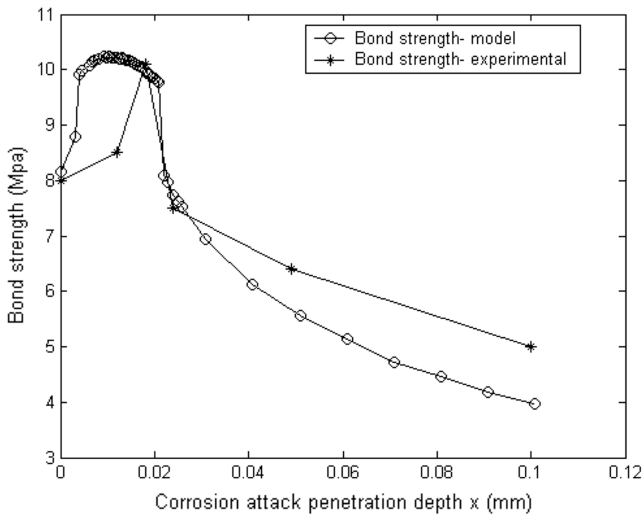


Fig. 6 Comparison of test results of Mangat and Elgarf (1999) and model

Two deformed bars, each of 10 mm diameter and 1100 mm length, were located symmetrically at a spacing of 50 mm center to center. A concrete cover of 25 mm to the center of reinforcement was provided. The compressive strength of the concrete after 28 days was 45 $N/mm^2$, with 1.0 $N/mm^2$ standard deviation. The degree of corrosion in the experiment is defined as 2 $RT$/d% (% reduction in rebar diameter), where $R$ is the corrosion in 'mm/year' and $T$ is the time in 'year' since the initiation of corrosion. Corrosion cracking occurred when the degree of corrosion increased from 0.4% to 0.5%. The corresponding attack penetration depth $x$ is approximately 0.020~0.025 mm. When the volume ratio $n$ is taken as 2.0, the calculated attack penetration depth $x_{cr}$ is 0.0209 mm. The calculated results are compared with the test results, see Fig. 6.

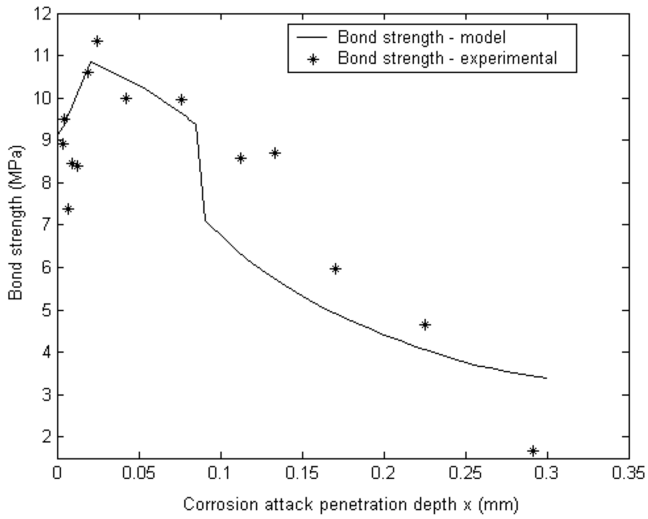


Fig. 7 Comparison of test results of Zhao and Jin (2002) and model

### *5.3 Comparison with test results of Zhao and Jin (2002)*

Another experiment is taken from the test of Zhao and Jin (2002). Pullout test was conducted on 100 mm cubic concrete specimen with 12 mm diameter deformed bar embedded centrally. The average compressive strength of the concrete cubes after 28 days was 22.13 MPa. Corrosion was determined by applying Faraday's law. The calculated results are compared with the test results, see Fig. 7.

## 6. Conclusions

In this paper, bond strength for corroded reinforcement is theoretically modeled. Firstly, the bar-concrete pressure for corroded bars is modeled. Before corrosion cracking, the maximum pressure $p(x)$ for corroded bars is taken as the maximum bursting capacity for noncorroded bars (Coronelli 2002), and the softening behaviour of concrete is considered in evaluating the maximum bursting capacity for noncorroded bars; after corrosion cracking, the residual confinement pressure is calculated in association with different corrosion levels. Secondly, corrosion pressure is evaluated by treating the cracked concrete as an orthotropic material before and after corrosion cracking. The corresponding methodology, originally proposed by Pantazopoulou and Papoulia (2001), is modified by using the equilibrium condition for the cracked part to calculate the unknown crack front $R_i$ at different corrosion levels. Finally, a model, which is originally proposed by Cairns and Abdullah (1996) and modified by Coronelli (2002) to take into account the effect of corrosion, is used to evaluate bond strength for corroded bars for splitting bond failure.

In order to evaluate the maximum bursting capacity for noncorroded bars, the methodology, originally suggested by Tepfers (1979), where a thick-walled cylinder is exposed to internal radial pressure, is still used to consider the softening behaviour of concrete. Smeared cracking and constant radial displacement are assumed in partly cracked concrete. The calculated relative maximum pressure $p_{\max}/f_{ct}$ is compared with Tepfers' classic solutions. The proposed model falls in between the partly cracked elastic stage and the plastic stage as pointed out by Tepfers.

Corrosion pressure before corrosion cracking is evaluated by treating the cracked concrete as an orthotropic material and sound concrete as an isotropic material. Boundary conditions are different from those used by Pantazopoulou and Papoulia (2001); and an equilibrium condition for the cracked part is added to calculate the unknown crack front $R_i$ at different corrosion levels. The calculated attack penetration depth $x_{cr}$ at the stage of concrete splitting reproduces the experimental results well.

Bond strength for corroded reinforcement is calculated and compared with test results. Bond strength increases at low corrosion levels, and then maximum bond strength occurs at a critical corrosion level, and finally decreases with increasing corrosion levels. There are some difference between the calculated results and test results, the causes of which are believed to lie in (1) unknown geometric characteristics of deformed bar used in the corresponding tests; (2) empirical formulae of coefficient friction $\mu(x)$ and adhesion strength $f_{coh}(x)$ (Coronelli 2002).

This analysis opens the way to study the mechanical behaviour of RC members with corroded reinforcement theoretically, taking into account the deterioration of bond strength with increasing degrees of corrosion levels.

## Acknowledgements

The authors gratefully acknowledge the support provided by the National Key Basic Research and Development Program (973 Program) No. 2002CB412709.

## References

Almusallam, A.A. (2001), "Effect of degree of corrosion on the properties of reinforcing steel bar", *Constr. Build. Mater.*, **15**, 361-368.

Al-Sulaimani, G.J., Kaleemullah, M., Basunbul, I.A. and Rasheeduzzafar (1990), "Influence of corrosion and cracking on bond behaviour and strength of reinforced concrete members", *ACI Struct. J.*, **87**(2), 220-231.

Amleh, L. and Mirza, S. (1999), "Corrosion influence on bond between steel and concrete", *ACI Struct. J.*, **96**(3), 415-423.

Andrade, C., Alonso, C. and Molina, F.J. (1993), "Cover cracking as a function of bar corrosion: Part I-Experimental test", *Mater. Struct.*, **26**, 453-464.

Auyeung, Y., Balaguru, P. and Chung, L. (2000), "Bond behaviour of corroded reinforcement bar", *ACI Mater. J.*, **97**(2), 214-221.

Cabrera, J.G. and Ghoddoussi, P. (1992), "The effect of reinforcement corrosion on the strength of the steel/concrete 'Bond'", *Proc. on Int. Conf. "Bond in Concrete"*, Latvia, 11-24.

Cairns, J. and Abdullah, R.B. (1996), "Bond strength of black and epoxy-coated reinforcement − A theoretical approach", *ACI Mater. J.*, **93**(4), 362-369.

Coronelli, D. (2002), "Corrosion cracking and bond strength modeling for corroded bar in reinforced concrete", *ACI Struct. J.*, **99**(3), 267-276.

Gambarova, P.G., Rosati, G.P. and Schumm, C. (1994), "An elasto-cohesive model for steel-concrete bond", *In Proc. of the Europe-US Workshop on Fracture and Damage in Quasibrittle Structures*, Edited by Bazant, Z.P., Bittnar, Z., Jirasek, M. and Mazars, J., Prague, 557-566.

Gambarova, P.G. and Rosati, G.P. (1997), "Bond and splitting in bar pull-out: behavioural laws and concrete cover role", *Mag. Concr. Res.*, **49**(179), 99-110.
Giuriani, E., Plizzari, G. and Schumm, C. (1991), "Role of stirrups and residual tensile strength of cracked concrete on bond", *J. Struct. Eng.*, **117**(1), 1-18.
Hsu, T.T.C. (1996), "Toward a unified nomenclature for reinforced concrete theory", *J. Struct. Eng.*, **122**(3), 275-283.
Lundgren, K. (2002), "Modelling the effect of corrosion on bond in reinforced concrete", *Mag. Concr. Res.*, **54**(3), 165-173.
Mangat, P.S. and Elgarf, M.S. (1999), "Bond characteristics of corroding reinforcement in concrete beams", *Mater. Struct.*, **32**, 89-97.
Molina, F.J., Alonso, C. and Andrade, C. (1993), "Cover cracking as a function of rebar corrosion: Part 2-Numerical model", *Mater. Struct.*, **26**, 532-548.
Nielsen, C.V. and Bicanic, N. (2002), "Radial fictitious cracking of thick-walled cylinder due to bar pull-out", *Mag. Concr. Res.*, **54**(3), 215-221.
Noghabai, K. (1994), "Environmental effects on bond in reinforced concrete structures", *Proc. of the 7th Int. Conf. Durability of Building Materials and Components 7 (Volume one)*, Stockholm, Sweden, 605-614.
Olofsson, T., Noghabai, K., Ohlsson, U. and Elfgren, L. (1995), "Anchorage and bond properties in concrete", *Fracture of Brittle, Disordered Material-Concrete, Rock and Ceramics*, Edited by. Baker, G., Karihaloo, B.L., UK: E & FN Son, Chapman & Hall, 525-543.
Pantazopoulou, S.J. and Papoulia, K.D. (2001), "Modeling cover-cracking due to reinforcement corrosion in RC structures", *J. Eng. Mech.*, **127**(4), 342-351.
Plizzari, G.A., Deldossi, M.A. and Massimo, S. (1998), "Transverse reinforcement effects on anchored deformed bar", *Mag. Concr. Res.*, **50**(2), 161-177.
Reinhardt, H.W. and Van Der Veen, C. (1992), "Splitting failure of a strain-softening material due to bond stresses", *In Applications of Fracture Mechanics to Reinforced Concrete*, edited by Elsevier Applied Science Publishers, 333-346.
Stanish, K., Hooton, R.D. and Pantazopoulou, S.J. (1999), "Corrosion effects on bond strength in reinforced concrete", *ACI Struct. J.*, **96**(6), 915-922.
Tepfers, R. (1979), "Cracking of concrete cover along anchored deformed reinforcing bar", *Mag. Concr. Res.*, **31**(106), 3-12.
Zhao, Y.X. and Jin, W.L. (2002), "Test study on bond behavior of corroded steel bar and concrete", *China J. of Zhejiang University (Eng Sci)*, **36**(4), 352-356.

## Appendix: $N \times N$ tridiagonal system of equations $[K][u_r] = [B]$

$$\left[\underset{N\times N}{K}\right] = \begin{bmatrix} K_{11} & K_{12} & 0 & 0 & \dots & \dots & 0 \\ K_{21} & K_{22} & K_{23} & 0 & \dots & \dots & 0 \\ 0 & \dots & \dots & \dots & \dots & \dots & 0 \\ 0 & 0 & K_{ii-1} & K_{ii} & K_{ii+1} & 0 & 0 \\ 0 & \dots & \dots & \dots & \dots & \dots & 0 \\ 0 & 0 & \dots & 0 & K_{N-1N-2} & K_{N-1N-1} & K_{N-1N} \\ 0 & 0 & 0 & \dots & 0 & K_{NN-1} & K_{NN} \end{bmatrix} \tag{A1}$$

where

$$K_{11} = \left(\frac{2}{h^2} + \frac{1}{r_1^2}\frac{E_{\theta,1}}{E_{r,1}}\right) \qquad K_{12} = -\left(\frac{1}{h^2} + \frac{1}{2r_1 h}\right)$$

$$K_{ii-1} = -\left(\frac{1}{h^2} - \frac{1}{2r_i h}\right) \qquad K_{ii} = \left(\frac{2}{h^2} + \frac{1}{r_i^2}\frac{E_{\theta,i}}{E_{r,i}}\right) \qquad K_{ii+1} = -\left(\frac{1}{h^2} + \frac{1}{2r_i h}\right) \quad i = 2, \dots, N-1$$

$$K_{NN-1} = -\frac{2}{h^2} \qquad K_{NN} = \frac{2}{h^2} + \frac{1}{r_N^2}\frac{E_{\theta,N}}{E_{r,N}} + \left(\frac{1}{h^2} + \frac{1}{2r_N h}\right) \cdot \frac{2h}{\nu_{r\theta,N} r_N}$$

$$[u_r]^T = [u_{r,1}, u_{r,2}, u_{r,3}, \ldots, u_{r,N}] \tag{A2}$$

$$[B] = \left[\frac{(n-1)(2R_0x - x^2)}{R_i + R_0} \cdot \left(\frac{1}{h^2} - \frac{1}{2r_1 h}\right), 0, 0, \ldots, a_N\right] \tag{A3}$$